U.S. DEPARTMENT OF ENERGY | Office of Science

DOE/SC-ARM-TR-215

First ARM Aerosol Chemical Speciation Monitor Users' Meeting Report

T Watson
Q Zhang
T Onasch
C Flynn
A Aiken
P Croteau
L Williams

June 2018

ARM

DISCLAIMER

DOE/SC-ARM-TR-215

First ARM Aerosol Chemical Speciation Monitor Users' Meeting Report

T Watson, Brookhaven National Laboratory
A Aiken, Los Alamos National Laboratory
Q Zhang, University of California, Davis
P Croteau, Aerodyne Research, Inc.
T Onasch, Aerodyne Research, Inc.
L Williams, Aerodyne Research, Inc.
C Flynn, Pacific Northwest National Laboratory

June 2018

Work supported by the U.S. Department of Energy,
Office of Science, Office of Biological and Environmental Research

Executive Summary

The first U.S. Department of Energy (DOE) Atmospheric Radiation Measurement (ARM) user facility aerosol chemical speciation monitor (ACSM) users' meeting was held on April 11-13, 2017, at Aerodyne Research, Inc. in Billerica, Massachusetts, to discuss the Southern Great Plains (SGP) atmospheric observatory ACSM data quality and establish best practices for data collection and processing. The participants examined six years of calibration and processed data. Specific issues raised by data users were addressed and case studies from two field experiments were examined. The most recent data from the ACSM installed in the newly commissioned SGP ARM Mobile Facility 7 (AMF7) were also evaluated. The participants recommended that the SGP ACSM data be reprocessed using calibration values averaged over the history of SGP ACSM calibrations. They also recommended that the data quality be evaluated by comparing (1) observed versus predicted particulate ammonium (NH_4^+) mass loadings, and (2) ACSM mass loadings versus mass loadings calculated from particle size and light scattering data. The contents of the datastreams from the ACSM were defined based on ARM requirements and the necessary tasks to implement these recommendations were assigned to the mentor and the instrument manufacturer.

Some of the recommendations were implemented for the SGP data and are presented in this report. Data from two ARM sites located in marine environments were also analyzed. These analyses as well as instrument intercomparisons have led to further questions about data treatment. These will be addresses in the second users' meeting scheduled for the summer of 2018.

Acronyms and Abbreviations

ACSM	aerosol chemical speciation monitor
ACTRIS	Aerosols, Clouds, and Trace Gas Research Infrastructure
ADC	ARM Data Center
ALC-IOP	aerosol life cycle intensive operational period
AMF	ARM Mobile Facility
AMS	aerosol mass spectrometer
AN	ammonium nitrate
AOS	aerosol observing system
ARM	Atmospheric Radiation Measurement
AS	ammonium sulfate
ASI	Ascension Island
BC	black carbon
BNL	Brookhaven National Laboratory
CDCE	composition-dependent collection efficiency
CE	collection efficiency
CPC	condensation particle counter
DMA	differential mobility analyzer
DOE	U.S. Department of Energy
DQO	Data Quality Office
ENA	Eastern North Atlantic
HEPA	high-efficiency particulate air
HI-SCALE	Holistic Interactions of Shallow Clouds, Aerosols, and Land-Ecosystems
HR-ToF-AMS	high-resolution, time-of-flight, aerosol mass spectrometer
IOP	intensive operational period
MAOS	mobile aerosol observation system
NIST	National Institute of Standards and Technology
OACOMP	Organic Aerosol Component VAP
PILS	particle-into-liquid sampler
PMF	Principal Matrix Factorization
PNNL	Pacific Northwest National Laboratory
QA	quality assurance
Q-ACSM	quadrupole aerosol chemical speciation monitor
QC	quality control
SBIR	Small Business Innovation Research
SGP	Southern Great Plains
SMPS	scanning mobility particle sizer
TDMA	tandem differential mobility analyzer
TMA	trimethylamine
ToF-ACSM	time-of-flight aerosol chemical speciation monitor
UHSAS	ultra-high-sensitivity aerosol spectrometer
VAP	value-added product

Contents

Figures

Tables

1.0 Motivation for Users' Meeting

The first ARM aerosol chemical speciation monitor (ACSM) users' meeting was held at Aerodyne Research, Inc. in Billerica, Massachusetts, April 11-13, 2017, to address questions raised by several investigators using ACSM data, particularly from the long-term observations made at ARM's Southern Great Plains atmospheric observatory in Lamont, Oklahoma. The purpose of this meeting was to establish best practices for instrument operation and data processing. The meeting focused on evaluating the quality of the historical data from six years of operation of the ACSM at SGP, determining the necessary calibration frequency, defining diagnostic tests that can be applied by the ARM Data Quality Office to automatically evaluate the ACSM data, and establishing the necessary parameters that should be included in the ACSM datastream.

2.0 Data Processing/Analysis

2.1 Concentration Calculations

The Aerodyne Igor Pro-based ACSM data analysis software calculates the concentration of particulate sulfate, ammonium, chloride, nitrate, and organics using the equation:

$$C_s = \left[\left(\frac{1}{CE * \ * RIEs * RF_{NO_3}}\right)\sum_{all\ i}\frac{IC_{s,i}}{T_{m/z}}\right] * \left(\frac{AB_{ref}}{AB_{meas}}\right)\P$$

Where:

$C_s \equiv$ The mass concentration of species s ($\mu g\, m^{-3}$)

$CE \equiv$ The ACSM collection efficiency of particulate mass

$RIE_s \equiv$ The relative ionization efficiency of species s $\left(\frac{RF_s}{RF_{NO3}}\right)$

$RF_{NO_3} \equiv$ The response factor to particulate nitrate (amps $/\mu g\, m^{-3}$)

$IC_{s,i} \equiv$ The sum of the ion currents (amps) for each of the molecular fragments formed by species s

$T_{m/z} \equiv$ Mass-to-charge-dependent transmission efficiency of mass spectrometer

$AB_{meas} \equiv$ Measured air beam (m/z 28) (amps)

$AB_{ref} \equiv$ Reference air beam (m/z 28) for a given sample flowrate (amps)

The nitrate response factor (RF_{N03}), the relative ionization efficiency of ammonium ($RIE_{NH4} = RF_{NH4}/RF_{NO3}$), and sulfate ($RIE_{SO4}$) are measured directly when the instrument is calibrated. Other relative ionization efficiencies for particulate organics and chlorides are determined based on measurements obtained using the Aerodyne aerosol mass spectrometer (AMS) and published in the peer-reviewed literature (Alfarra et al. 2004). The mass-dependent transmission efficiency ($T_{m/z}$) of the mass spectrometer (the SGP ACSM has a quadrupole mass spectrometer) can be directly measured and the

measured value or the default transmission efficiency can be used in the data processing. Uncertainties and assumptions are associated with most of these terms.

Variations in sample flow and detector response are corrected for by using the ratio of the air beam signal (N_2 at m/z 28) measured at each data point to a reference value determined at the time of calibration.

The term $\sum_{all\ i} IC_{s,i}/T_{m/z}$ represents the sum of the signals at all m/z that are fragments of the species of interest. These data are defined in a fragmentation table that has been compiled based on published AMS and ACSM measurements (Allan et. al. 2004; also see 2.5 Fragmentation).

2.2 Calibration

Calibration is performed by introducing ammonium nitrate (AN) and ammonium sulfate (AS) into the instrument as size-selected 300-nm-diameter particles at a range of number concentrations. Particle number is controlled using a dilution bridge, particle diameter is controlled with a differential mobility analyzer (DMA), and particle number is measured using a condensation particle counter (CPC). The calibration process should be done in the same way as ambient data acquisition measuring one cycle of filter signal, and one of sample signal, and calculating the difference between the two. The difference data are used to calculate the NO signal in amperes as a function of the input mass loading in μgm^{-3} calculated from the particle diameter, number concentration, material density, and shape factor, yielding the NO_3 response in amps/μgm-3 (RF_{NO3}). The relative ionization efficiency of NH_4 to NO_3 (RIE_{NH4}) is determined from the NH_4NO_3 data. The $(NH_4)_2SO_4$ data give the NH_4-to-SO_4 relative ionization efficiency, which can be combined with RIE_{NH4} to determine the SO_4-to-NO_3 relative ionization efficiency (RIE_{SO4}). This sequence is implemented in the latest generation of data acquisition software that is currently installed on all DOE Q-ACSMs. This sequence is particularly important for ammonium sulfate calibration, which should be done in sampling mode with filter, sample, and difference because of buildup of SO_4 background in the instrument. In the past, the AN calibration has been done with sample data (i.e., no subtraction of filter), but for consistency it should also be performed with difference data.

2.3 Collection Efficiency (CE)

The default CE of 0.5 should be used for the automatically calculated data. A composition-dependent collection efficiency (CDCE), based on the work in Middlebrook et al. 2012, can be used when the aerosol composition is dominated by nitrate or acidic sulfate (Section 7.1). Automating the application of the CDCE is difficult because the ammonia data tend to be noisy and judgement must be used to smooth the correction factor before application.

2.4 Air Beam

The detector sensitivity decreases over time, particularly if the detector has been exposed to atmospheric pressure (Section 5.1). The air beam correction factor is used to account for changes in detector sensitivity from this and other causes. The correction factor is the ratio of the air beam signal at the time of calibration to the air beam signal at the time of data collection. Signals at all m/z are multiplied by this factor. An example is shown in Figure 1. The large change in the correction was caused by an inadvertent change in quadrupole polarity.

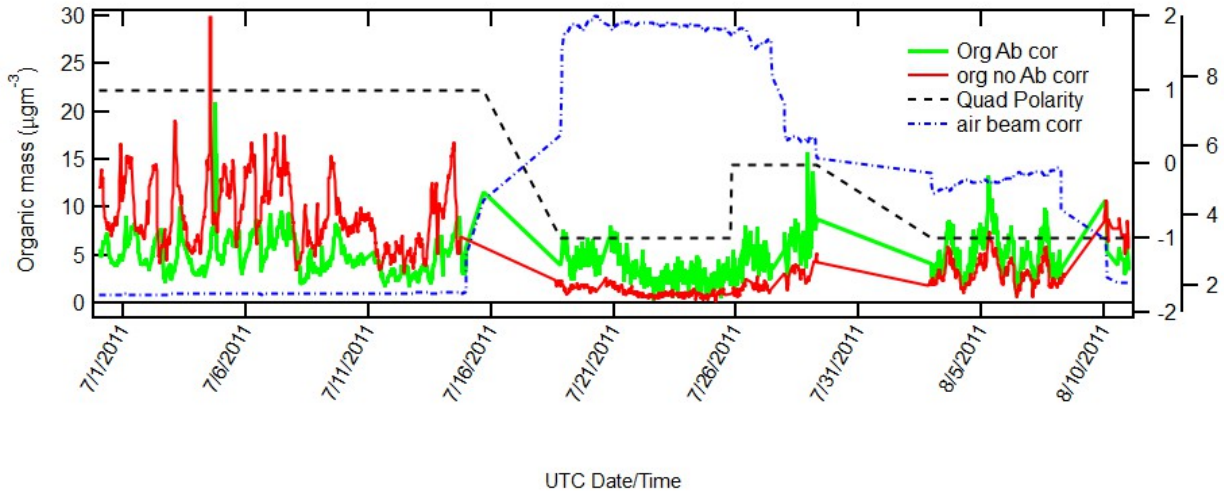

Figure 1. Air beam correction factor applied across step change in detector sensitivity resulting from change in quadrupole polarity. Traces are air beam correction factor (blue dashed), corrected organic signal (green), uncorrected organic signal (red), and quadrupole polarity (black dashed).

This polarity change significantly decreased the transmission efficiency of the quadrupole uniformly over all m/z; however, the air beam correction factor compensated for this decrease in sensitivity. As a result, there is no step change in the corrected data, although the signal-to-noise ratio is lower because of the large multiplicative factor.

2.5 Fragmentation

In the ACSM, the vaporization process causes thermal decomposition of the molecules that comprise the aerosol and electron impact ionization causes further fragmentation. The fragmentation pattern is reproducible and has been identified for many species using the AMS. In ambient aerosols there are a mixture of species that may have similar fragments as well as isotopes of some of the constituent atoms. The fragmentation table is used to calculate the contributions to the signal for a particular species and correct for interfering signals from other species. An example of the fragmentation table for the calculation of nitrate signal is given in Table 1. The major contributions to the nitrate signal are from the NO^+ fragment at m/z 30 and the NO_2^+ fragment at m/z 46. The signal at m/z 46 is assigned to nitrate without correction because the organic signal at this m/z is typically small based on high-resolution ambient AMS data. The organic contribution is subtracted at m/z 30. The signal at m/z 14 is calculated from the m/z 30 and 46 signals by adding fractions of the m/z 30 and 46 signal to account for the measured fragmentation patterns of NO^+ and NO_2^+. The natural isotopic abundance of ^{15}N, ^{17}O, and ^{18}O are used to calculate signals at m/z 31 and 32 from the NO^+ signal and at m/z 47 and 48 from the NO_2^+signal (Allan et al. 2004). The signal at m/z 63 is calculated from NO^+ and NO_2^+signal to account for the fraction of nitrate that does not fragment. The minus signs in front of the other species in the table represent subtraction of interfering signals caused by presence of these fragments from other compounds in the sample.

Table 1. Example of the fragmentation table for nitrate.

m/z	frag_nitrate
14	0.04*frag_nitrate[30],0.04*frag_nitrate[46]
30	30,-frag_organic[30]
31	0.00405*frag_nitrate[30]
32	0.002*frag_nitrate[30]
46	46
47	0.00443*frag_nitrate[46]
48	0.004*frag_nitrate[46]
63	1.5*0.002*frag_nitrate[30],0.002*frag_nitrate[46]

2.6 Ion Transmission

The transmission of ions through the quadrupole is mass dependent (Figure 2). The ion transmission correction factor is 1.0 from m/z 10 to m/z 50 and exhibits a sharp decrease to less than 0.5 at m/z 100 and even lower for higher m/zs. It is necessary to apply a mass-dependent correction, $T_{m/z}$, for m/z>50.

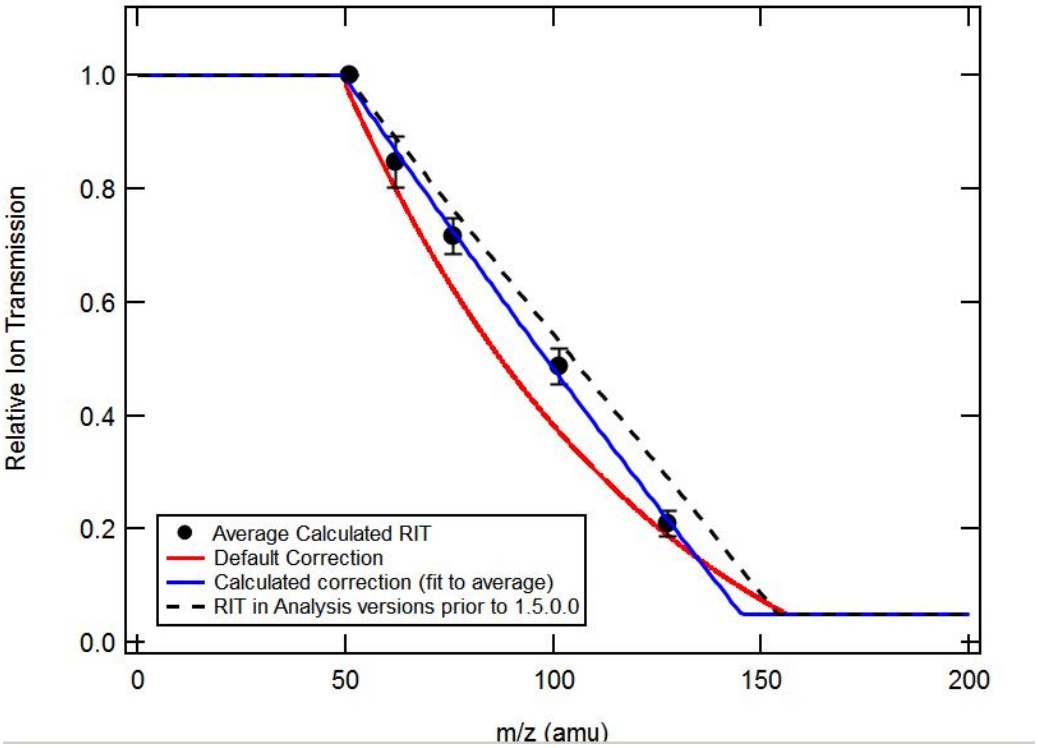

Figure 2. Default ion transmission and measured ion transmission.

The ACSM ion transmission is calculated by comparing the measured naphthalene peaks from an internal naphthalene source. The strongest signal is at the parent naphthalene peak is at m/z 128. The naphthalene peaks are compared to the National Institute of Standards and Technology (NIST) fragmentation pattern and normalized to the measured signal for the cluster of peaks around 50 using the assumption that transmission from 0-50amu is 100%. These data are used to determine the calculated ion transmission

correction as shown in Figure 2. In the analysis software, a default correction is applied on loading the data (red line in Figure 2), and the user may apply the calculated/fitted correction (blue line in Figure 2). In both the default and fitted correction case the fit is truncated to a flat line when the transmission reaches 0.05 so that the maximum correction is a factor of 20. This correction adds significant uncertainty to the measured intensity of ions at greater than 100 amu, suggesting that these signals should not be used for factor analysis. Although the correction is large, it has a minimal effect on the mass loading since typically only ~5% of mass measured is contained in fragments with m/z greater than 100. One exception is in the case of biomass burning plumes, which can have significant signal at m/zs greater than 100. The best biomass markers at m/z 60 and 73 are still available to characterize biomass aerosol. The default ion transmission efficiency works well. The difference between applying the default or measured RIT correction is relatively small. Use of the default ion transmission is recommended. For either transmission efficiency curve, the noise at high m/z increases significantly because of the high multiplicative factor.

2.7 Variations between Instruments in the Signal Observed at M/Z 44

Crenn et al. (2015) discussed the results of comparing 13 quadrupole ACSM (Q-ACSM) instruments and one ToF-ACSM, and one high-resolution, time-of-flight, aerosol mass spectrometer (HR-ToF-AMS) during the Aerosols, Clouds and Trace Gas Research Infrastructure (ACTRIS) Network intercomparison conducted in Paris in 2013. While the agreement in the mass loadings between the instruments was good, they reported that the mass spectra varied across systems. The variability was dominated by the fractional contribution of m/z 44 (CO_2^+) represented symbolically as *f*44. The signal at m/z 44 is consistent with the observations of oxygenation of the aerosol particles (Pieber et al. 2016). The current hypothesis about the origin of this variability is related to the history of the ACSM vaporizer. Systems that have encountered higher organics and/or black carbon loadings may develop a layer of char on the surface of the vaporizer. The char may then be oxidized by oxygen containing fragments to generate CO_2^+. The most common oxidant is the NO_2 evolved from the decomposition of NH_4NO_3 aerosol. This variability in measured fragmentation suggests that a commonly used parameterization that relies on *f*44 to calculate O:C and H:C of organic aerosol (Aiken et al. 2008) may not be applicable to ACSM (or AMS) data, depending upon the history of the vaporizer.

3.0 SGP Calibration History

The ACSM at SGP was put into service in 2011. Factory calibrations were performed in 2010 before shipment to SGP and in 2014 after factory service. No recorded calibrations occurred in the three years between these two. Quarterly calibrations were initiated in July 2015. The results of all available calibrations are given in Figure 3.

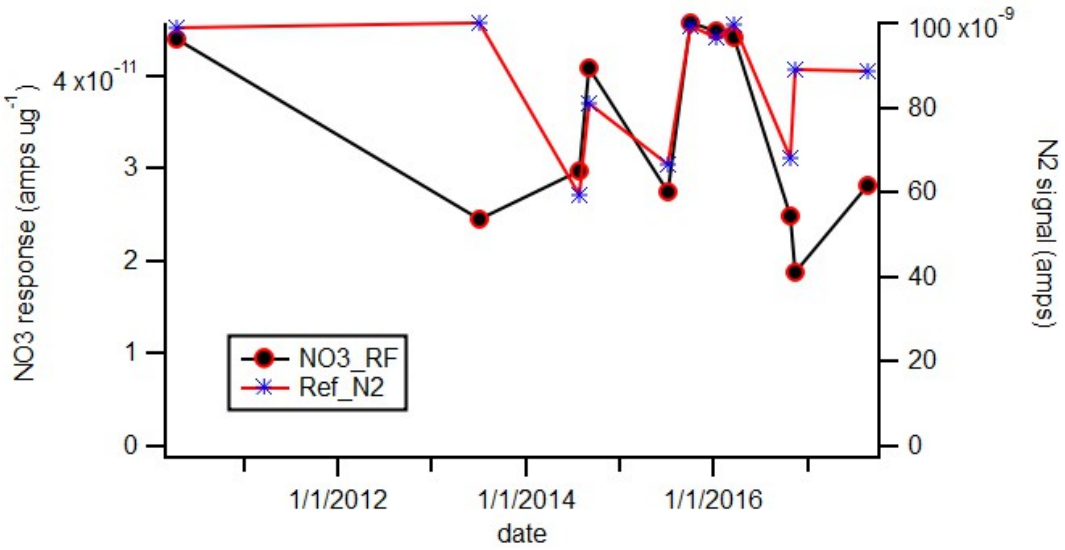

Figure 3. The nitrate response factor (RF_{NO3}) and reference air beam (Ref_N_2) versus time.

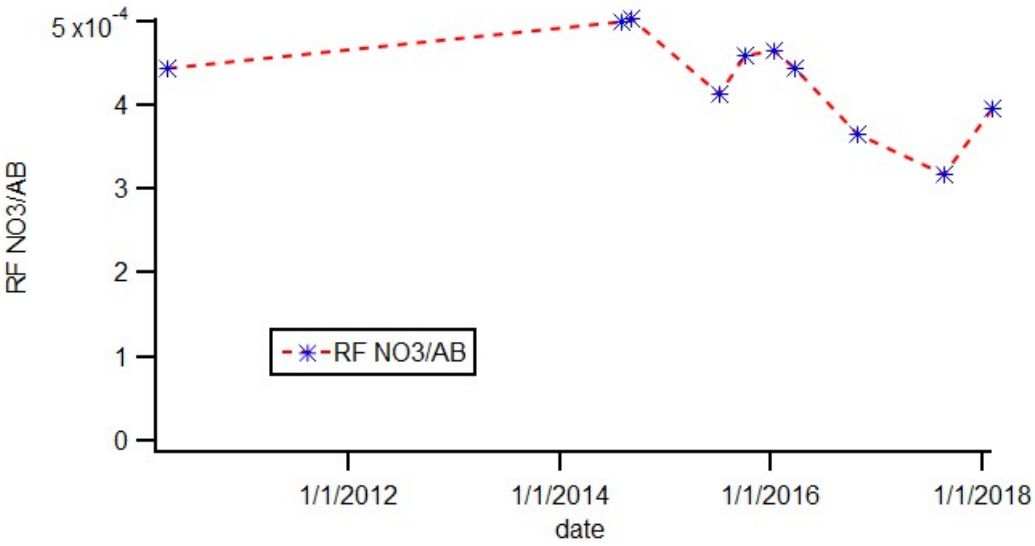

Figure 4. (RF_{NO3})/AB versus time. The values collected on 7/3/2013 and 11/15/2016 have been removed because of documented problems.

3.1 Examination of Calibration Stability Using Six Years of SGP Data

The participants came to several important conclusions after examination of the calibration history of the SGP ACSM. The successful calibrations are reasonably consistent over the seven-year history of the instrument at SGP. RF_{NO3}, RIE_{NH4}, and RIE_{SO4} values, when scaled by the value of the air beam at the time of calibration, are also consistent (Figure 4 and Table 2).

3.2 Conclusions

The average calibration across the history of the ACSM should be used in the data processing. Calibration is remarkably stable and calibration every six months is adequate. Deviation from the average should be used to assess the quality of the calibration. All the SGP ACSM data presented in Section 4 were reprocessed using the average values of RF NO_3, RIE NH_4, and SO_4 given in Table 2. The reference air beam used in the recalculation was determined using the average ratio of average of RF NO_3, 3.53e-11 divided by the average of Ref N_2, 4.29e-4, resulting in an average reference air beam value of 8.2e-8 amps.

Table 2. Calibration history of SGP ACSM collected over seven years of operation. The missing values on 7/3/2013 and 11/15/2016 are because of documented problems with the calibrations. "Stdev" is standard deviation. "rel stdev" is relative standard deviation.

Date	RF NO_3	RIE NH_4	RIE SO_4	Ref N_2	Ref NO_3/Ref N_2
4/14/2010	4.40E-11	5.60		9.90E-08	4.44E-04
7/3/2013					
8/1/2014	2.97E-11	6.19	0.82	5.95E-08	4.99E-04
9/3/2014	4.08E-11	7.09	1.07	8.11E-08	5.03E-04
7/7/2015	2.75E-11	7.33	0.70	6.66E-08	4.13E-04
10/6/2015	4.57E-11	5.77	1.03	9.94E-08	4.60E-04
1/14/2016	4.49E-11	6.39	0.91	9.65E-08	4.65E-04
3/22/2016	4.42E-11	7.76	1.05	9.97E-08	4.43E-04
10/25/2016	2.49E-11	4.28	0.65	6.80E-08	3.66E-04
11/15/2016					
8/24/2017	2.81E-11	5.13	0.60	8.86E-08	3.17E-04
2/5/2018	2.27E-11	5.40	0.52	5.74E-08	3.95E-04
Average	3.53E-11	6.09	0.82	8.16E-08	4.29E-04
Stdev	9.41E-12	1.08	0.21	1.73E-08	5.86E-05
rel stdev	0.27	0.18	0.26	0.21	0.14

4.0 SGP ACSM: Performance by Year from 2011 to 2016

4.1 2011: Issues and Resolutions

At some point in 2011, a Nafion dryer was added to the inlet of the instrument, but there is no record of installation. The addition of the dryer decreases the water content of the aerosol, which influences the collection efficiency. The effect on the data before this installation is unknown.

It appears that the critical orifice was changed and a 120-µm orifice installed in July 2011 as can be seen in the record of inlet pressure (Figure 1). There is a jump from 1.2 torr to 1.6 torr when this occurred. Since the air beam increases proportionally to the increase in inlet pressure, the air beam correction compensates for this change.

The quadrupole polarity was switched 2011-07-18 (Figure 1). This was discovered during examination of the data at the users' meeting. The polarization change resulted in a decrease in measured ion currents and a decrease in the signal-to-noise ratio. While the air beam correction compensates for the signal loss, signal-to-noise ratio is lower for the data obtained during this period.

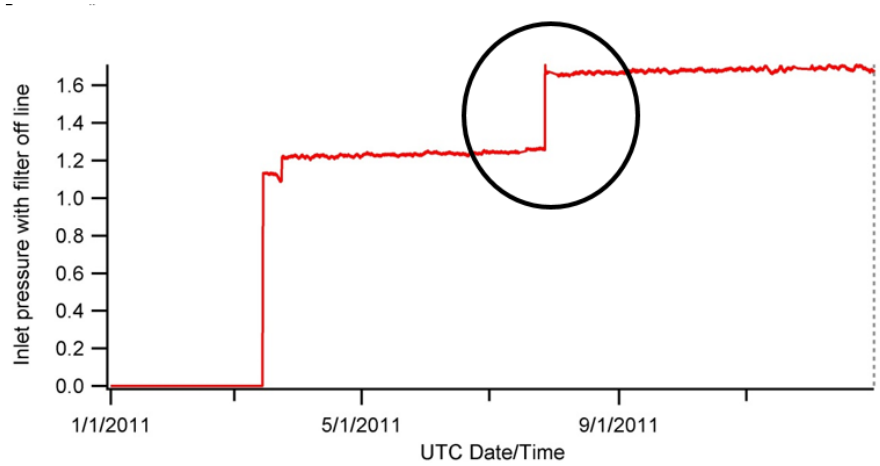

Figure 5. Pressure change with installation of the 120-µm critical orifice indicated with the black circle. The data at zero were collected before the data acquisition software was updated to collect inlet pressure data.

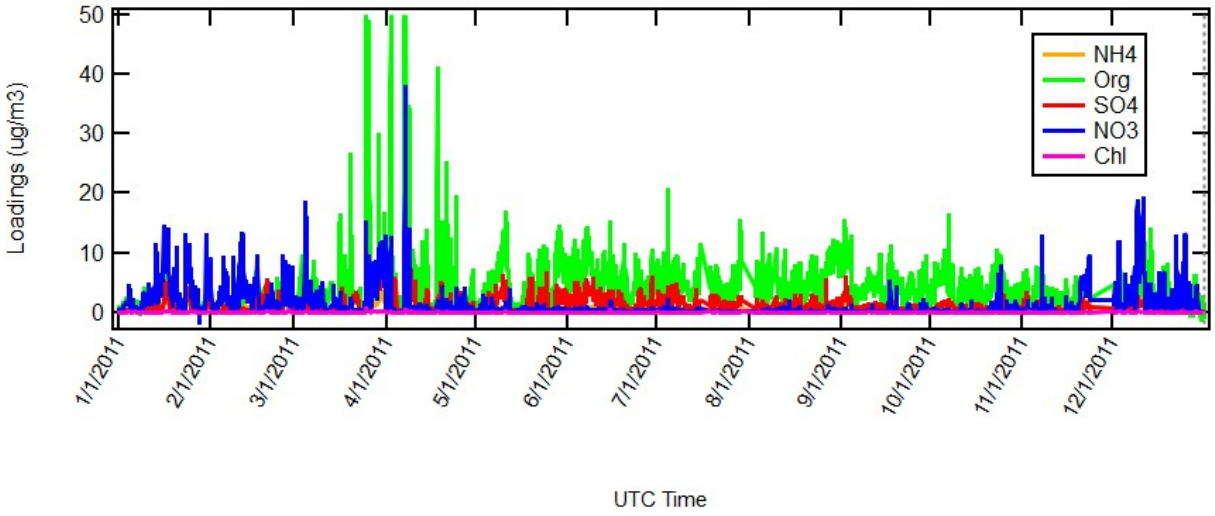

Figure 6. Time series of 2011 data processed using the average calibration values over the seven-year history of SGP ACSM operation. Y axis has been expanded to show detail, which cuts off the peak maxima in late May and April.

4.2 2012: Issues and Resolutions

The ACSM was removed from service and shipped to Aerodyne for replacement of a turbo pump service in 2012. There is no record of the results of any factory calibration during this service. A step change in the data occurred after the instrument was returned to service (Figure 7) because of an incorrect application of the air beam correction and was the motivation for the data reprocessing that was done by

the ARM mentor (Tom Watson) in 2015. The data were again reprocessed using the average calibration values given in Table 2. This reanalysis corrected the step jump (Figure 8).

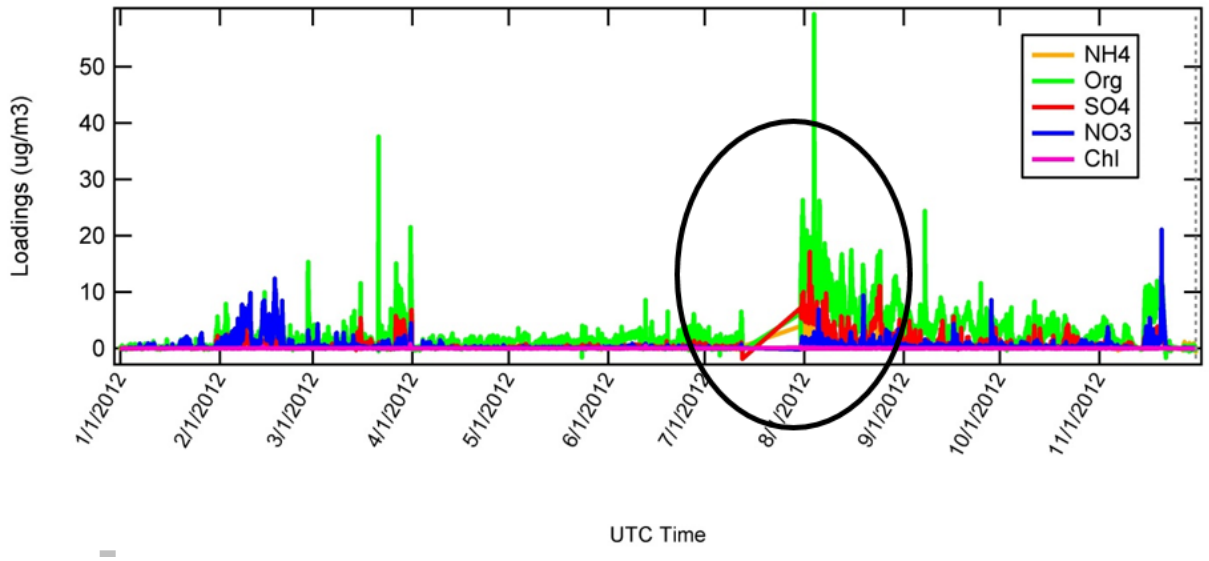

Figure 7. Step change in the original 2012 data after the instrument was returned to service. The step jump caused by incorrect application or the air beam correction is indicated by the black oval.

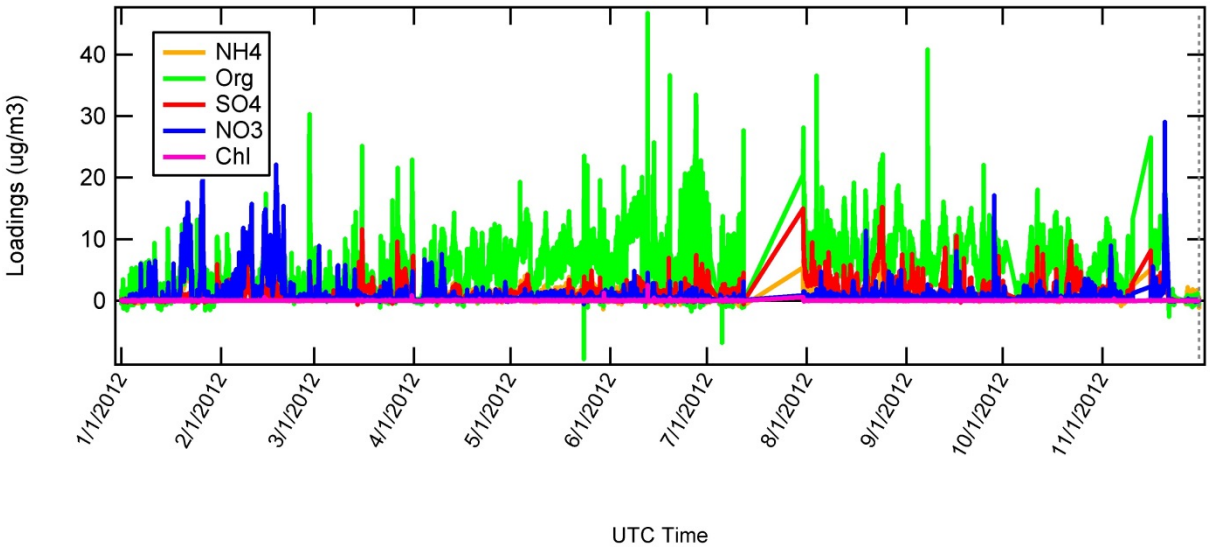

Figure 8. Time series of 2012 data processed using the average calibration values over the seven-year history of SGP ACSM operation. Use of the same value of the reference air beam across the data set eliminated the step jump.

4.3 2013: Issues and Resolutions

In 2013, there was an unsuccessful attempt to calibrate the instrument using the ARM calibration scanning mobility particle sizer (SMPS). Because of the inexperience of the ARM mentor, Watson, with this instrument, a stable CPC signal was not obtained. The 120-µm critical orifice was replaced during the

calibration attempt with a standard 100-µm orifice and the inlet pressure returned to normal operating levels. Processing the data with the average calibration values and application of the air beam correction eliminated the problem caused by the pressure difference. The time series of corrected data is presented in Figure 9.

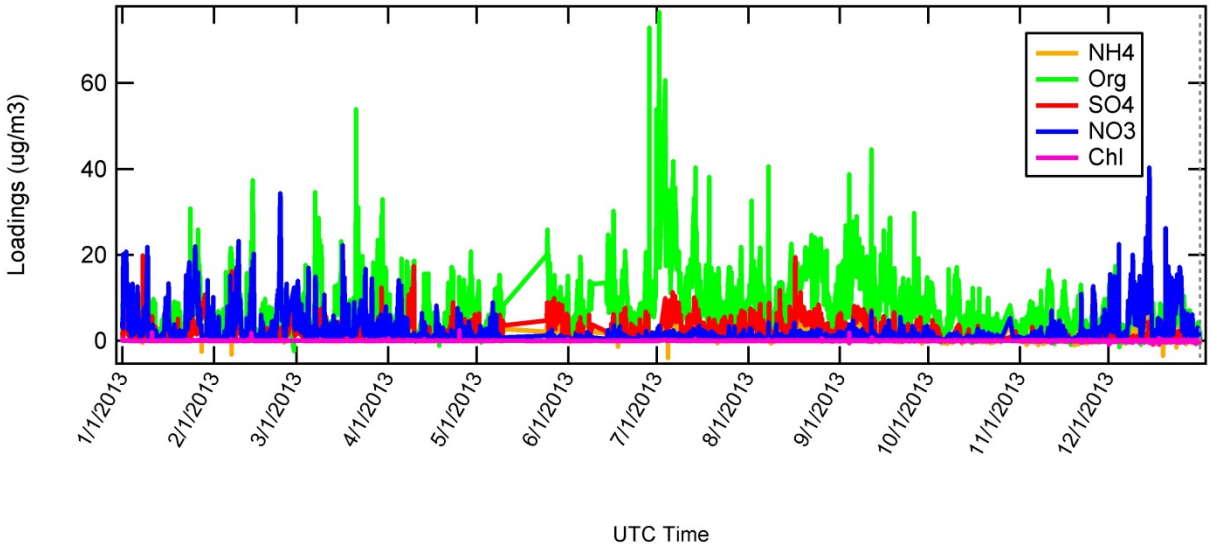

Figure 9. Time series of 2013 data processed using the average calibration values over the seven-year history of SGP ACSM operation.

4.4 2014: Issues and Resolutions

Many instrument problems occurred in 2014, including multiple turbo molecular pump failures, a filament failure, and a computer software lockup. This is apparent in the gap in the time series for 2014 from late May through early October (Figure 10). In August 2014, the instrument was returned to the factory for a pump replacement and was calibrated at this time. This was the first documented, reliable calibration since 2010.

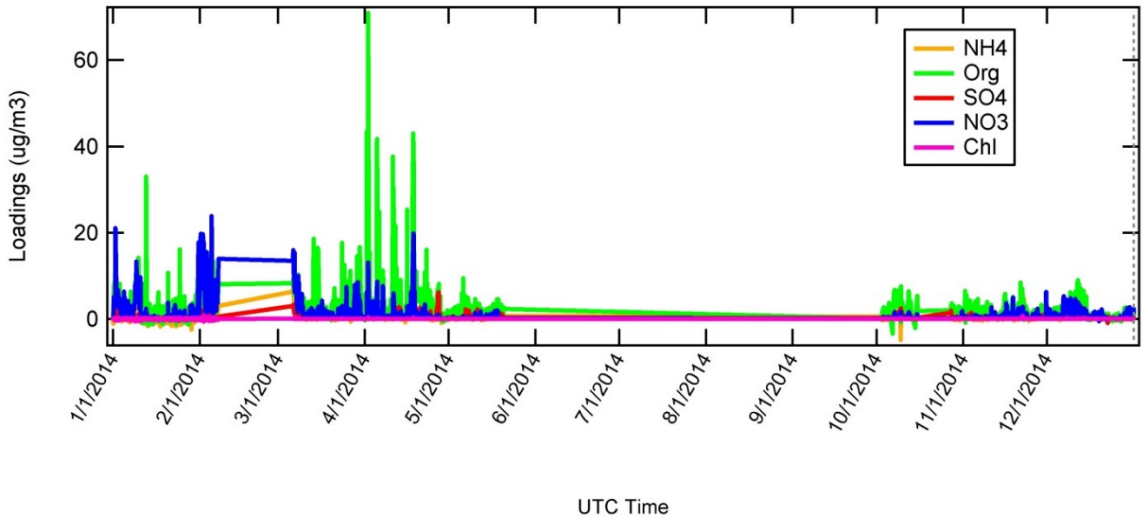

Figure 10. Time series of 2014 data processed using the average calibration values over the seven-year history of SGP ACSM operation.

4.5 2015: Issues and Resolutions

Quarterly calibrations were begun in 2015. These calibrations were performed with an experienced operator setting up and monitoring the SMPS. Calibrations from this time forward are, with two exceptions, reliable.

A bank of vacuum gauges was installed inside the building for all the aerosol observing system (AOS) pumps housed in the pump rack on 2015-08-11 to identify pump failures or other problems. After installation of a "Tee" fitting in the ACSM vacuum line, the inlet pressure dropped from 1.3 torr to 0.93 torr (Figure 11). A critical orifice that limited the flow past the instrument to approximately 3 lpm was inadvertently removed by the site operator during the installation of the gauge, which caused the low inlet pressure. The old Nafion dryer was removed and an Aerodyne inlet dryer system and sample pump were installed during the calibration on 2015-10-6, which corrected the problem. Figure 12 is the time series of the corrected data. Data from the period of the pressure problem were removed and flagged as incorrect in the Data Center.

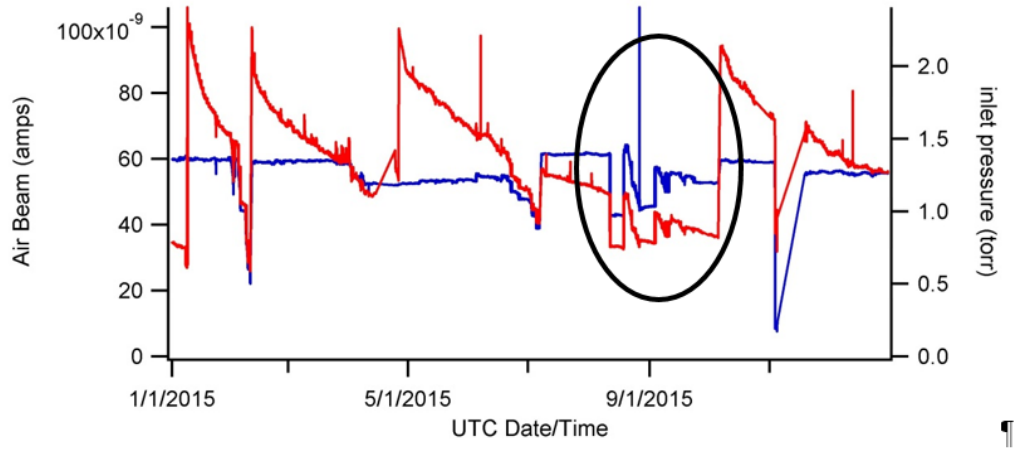

Figure 11. Time series of air beam (red) and inlet pressure (blue) for 2015. The sampling pump problem is indicated by the black oval.

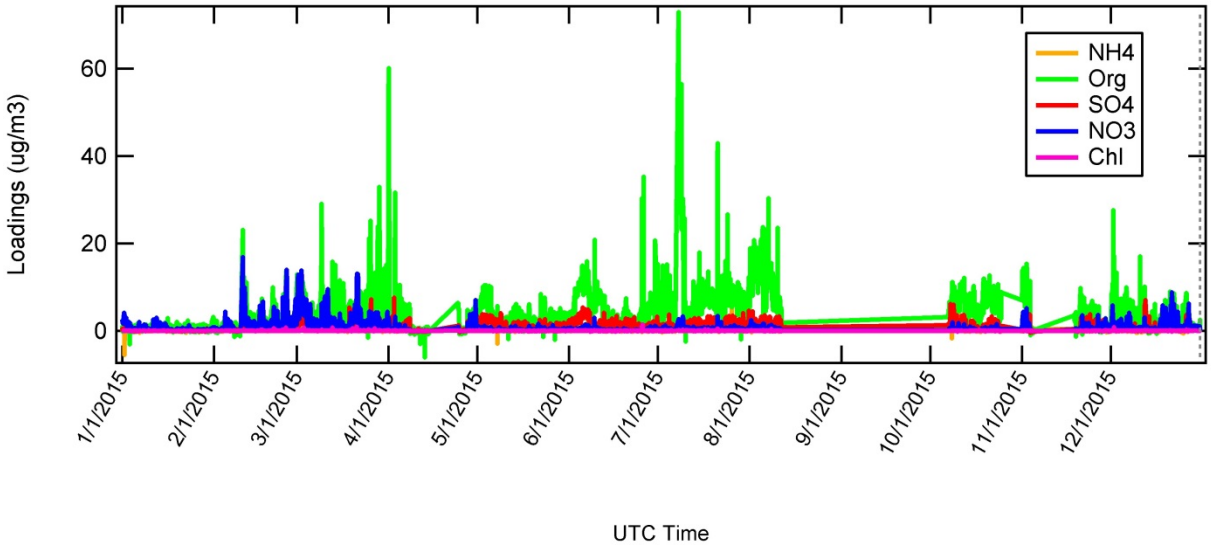

Figure 12. Time series of 2015 data processed using the average calibration values over the seven-year history of SGP ACSM operation.

4.6 2016: Issues and Resolutions

In 2016 several significant events occurred at SGP. The Holistic Interactions of Shallow Clouds, Aerosols, and Land-Ecosystems (HI-SCALE) field campaign was conducted in 2016 with intensive operation periods (IOPs) in April-May 2016 and again in September. The new ARM Mobile Facility 7 (AMF7) was installed in November. Prior to that, the ACSM was taken out of service and installed in the container at Brookhaven National Laboratory (BNL) before returning to SGP. This is apparent in the gap in the time series of the data (Figure 13). Additional instruments, including an SMPS and an ultra-high-sensitivity aerosol spectrometer (UHSAS), were added to the suite of instruments at the site.

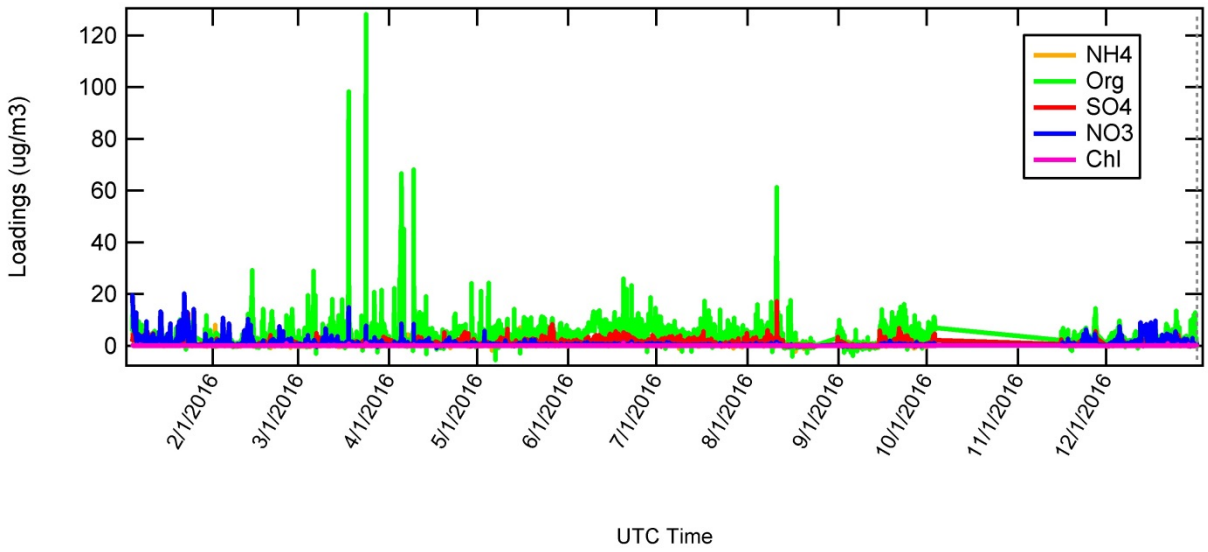

Figure 13. Time series of 2016 data processed using the average calibration values over the seven-year history of SGP ACSM operation.

5.0 Case Studies

5.1 Comparison of ACSM Mass Loading with UHSAS

The availability of the SMPS and UHSAS data made comparisons of ACSM mass loadings with the mass loadings calculated from these instruments for the period 2016-11-15 to 2017-01-31 possible. This analysis revealed discrepancies between mass loading calculated by integrating the measured size distribution and the mass loading measured by the ACSM.

Detector Sensitivity Change

During the comparisons of ACSM mass loading with UHSAS, the ACSM mentor, Watson, noticed changes in the ACSM detector sensitivity after the vacuum chamber was vented during the installation of a new turbo molecular pump. Examination of the air beam, oxygen, and naphthalene signals of the ACSMs at the Eastern North Atlantic site (ENA) and the site on Ascension Island (ASI) showed the same behavior in all three ARM quadrupole ACSMs. Detector sensitivity quickly decays after exposure to atmosphere by as much as a factor of 5 and takes 3 to 4 weeks to stabilize to a normal decay rate (Figure 14). Similar behavior occurs with the installation of a new detector. Despite the decay in sensitivity, each of the signals decays in tandem. The air beam factor corrects for this. The cause for this decay is in the detector. Channeltron electron multipliers such as those used in the ACSM have a clean-up period after exposure to atmospheric pressure characterized by an initial drop in gain due to gas molecules desorbing from the surface. This data indicates that this clean-up time can be significant in the ACSM system. If possible, calibration should not be performed until at least two weeks after a vent.

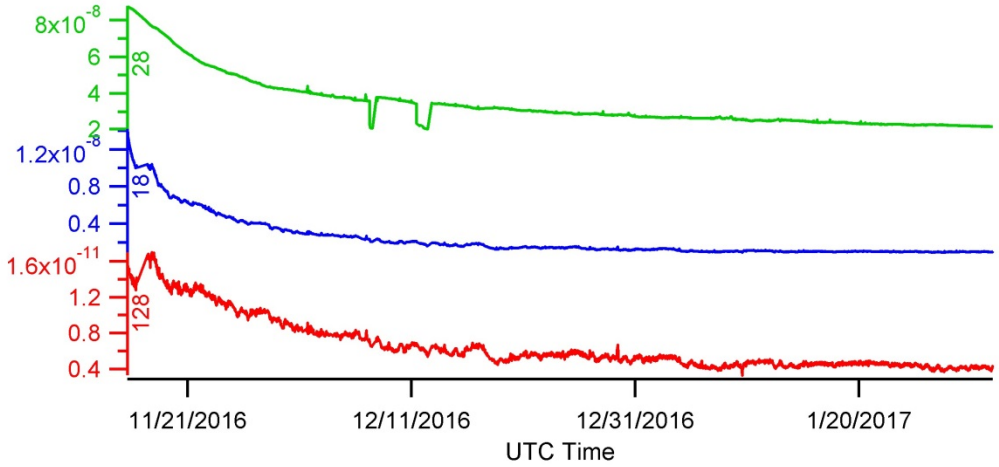

Figure 14. Time series of air beam (m/z 28, green), oxygen (m/z 18, blue), and naphthalene signals 2016-11-15 to 2017-01-31 showing a sharp decay in the detector sensitivity after exposure to atmospheric pressure.

The meeting participants also concluded that the secondary electron multipliers in two of the three DOE Quad-ACSMs are nearing the end of their service life and should be replaced soon. Locations, serial numbers, and current detector voltages are given in (Table 3).

Table 3. Current location, serial number, and detector voltage of DOE Quad-ACSM instruments.

Location	SN	SEM voltage
SGP	140.103	1918
ENA	140.107	2021
ASI	140.106	1428

5.2 HI-SCALE

Jerome Fast compared the data from ACSM, AMS, and SMPS collocated during the first IOP of the HI-SCALE field program conducted at SGP. He found that the data from all three instruments were well correlated but that the ACSM raw mass loadings, uncorrected for collection efficiency (CE), were less than that calculated from SMPS, or measured by AMS. The processed ACSM data was a factor of 2 higher than the raw ACSM data and the processed ACSM mass loadings were greater than either the AMS or the calculated SMPS mass loadings (Figure 15). This factor of 2 increase is a result of application of the CE correction.

Fast also found that the difference was composition dependent, suggesting that, apparently, applying a CE of 0.5 for all species was not correct. He calculated species-dependent correction factor using the AMS data. These factors brought the AMS and processed ACSM data into better agreement (Table 4).

Table 4. Correction factors calculated by Fast for HI-SCALE IOP 1 AMS and ACSM data.

Species	Calculated correction factor
Org	1.6
SO4	1.3
NO3	1.3
NH4	0.9

Several questions were raised about the Pacific Northwest National Laboratory (PNNL) treatment of the data at the users' meeting. These questions include:

- Did Fast calculate a CDCE for the ACSM from the AMS?
- Is the CDCE being defined as that which yields the best agreement between the ACSM and the AMS?
- Are these factors in addition to the default CE of 0.5? Or instead of the default CE?
- What is the density used to convert the SMPS data to mass loading?
- Was spike removal performed on the ACSM data by PNNL?
- How were the AMS mass loading data calculated?

The participants also were interested in seeing the AMS raw mass spectra. These will issues be discussed with Fast et al.

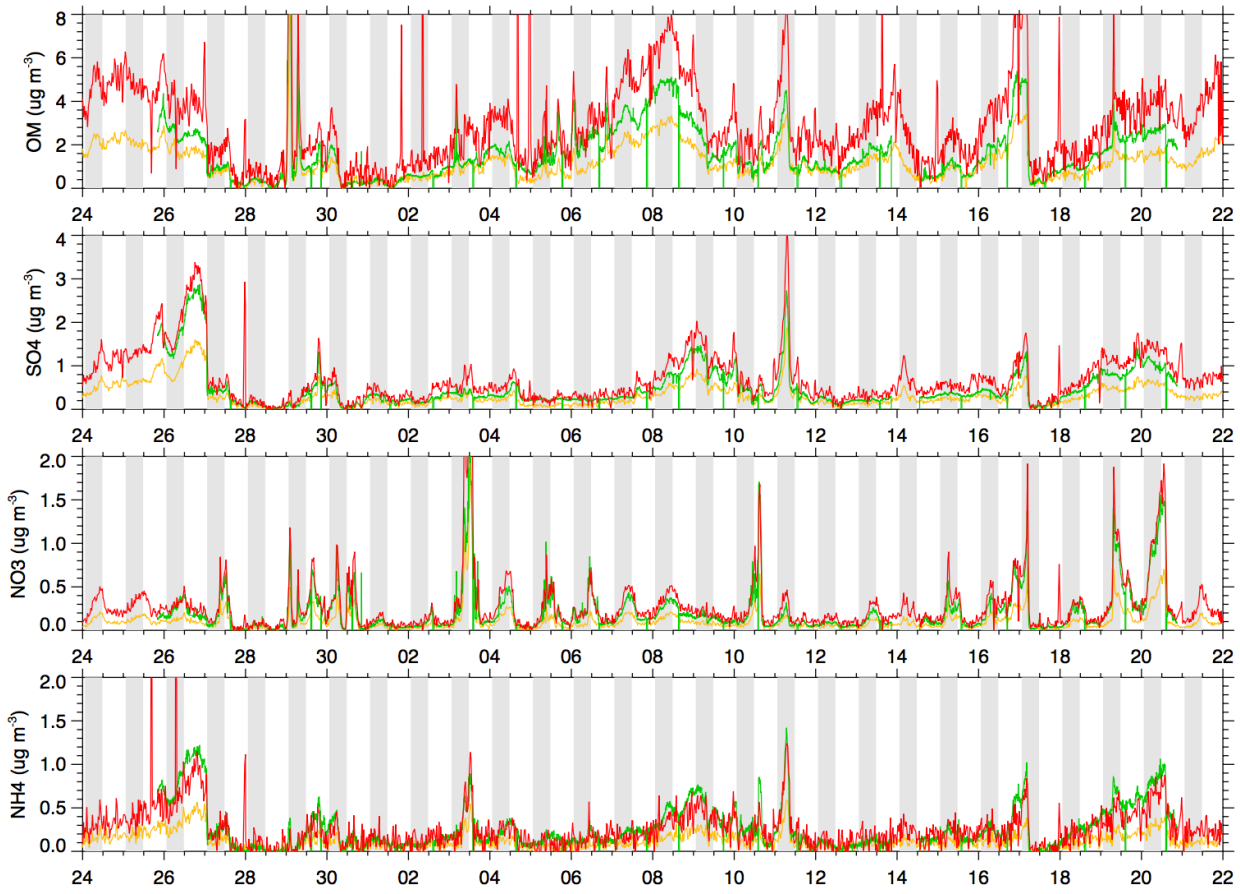

Figure 15. Time series of mass loading data from the ACSM before (gold) and after (red) mentor processing and the AMS data (green). Plots provided by Jerome Fast.

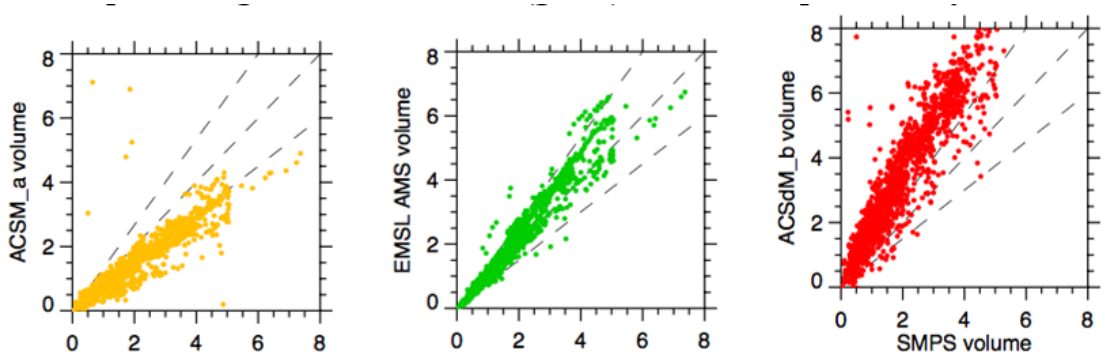

Figure 16. Correlation plots of volume calculated from ACSM raw data (yellow), AMS data (green), and ACSM processed data (red) versus volume calculated from SMPS data. Plots provided by Jerome Fast.

5.3 Data Issues Observed by Qi Zhang

5.3.1 Reprocessing of SGP Data

Qi Zhang analyzed the 1.5 years of original data acquired from SGP from November 2010 to June 2012 and developed the Organic Aerosol Component (OACOMP) value-added product (VAP) as a result. However, since the calibration values, air beam correction, and collection efficiency used in generating the archived data are unknown, the data were reprocessed in 2015 by Watson and sent to the Data Center in 2015. The new analysis applied the air beam correction and calibration data consistently over the time when there were no recorded calibrations. The values used in the reprocessing are given in Table 5. These are quite different than the values in Table 2.

Table 5. Values used in the Watson reprocessing of 2015.

RF NO_3	4.40E-11
air beam	9.90E-08
RIE NH_4	5.6
RIE SO_4	0.82
CE	0.5

The Zhang group compared the original data with the reprocessed data and discovered that there are differences as can be seen in Figure 17 and Table 6. The data have been reprocessed again using the average values.

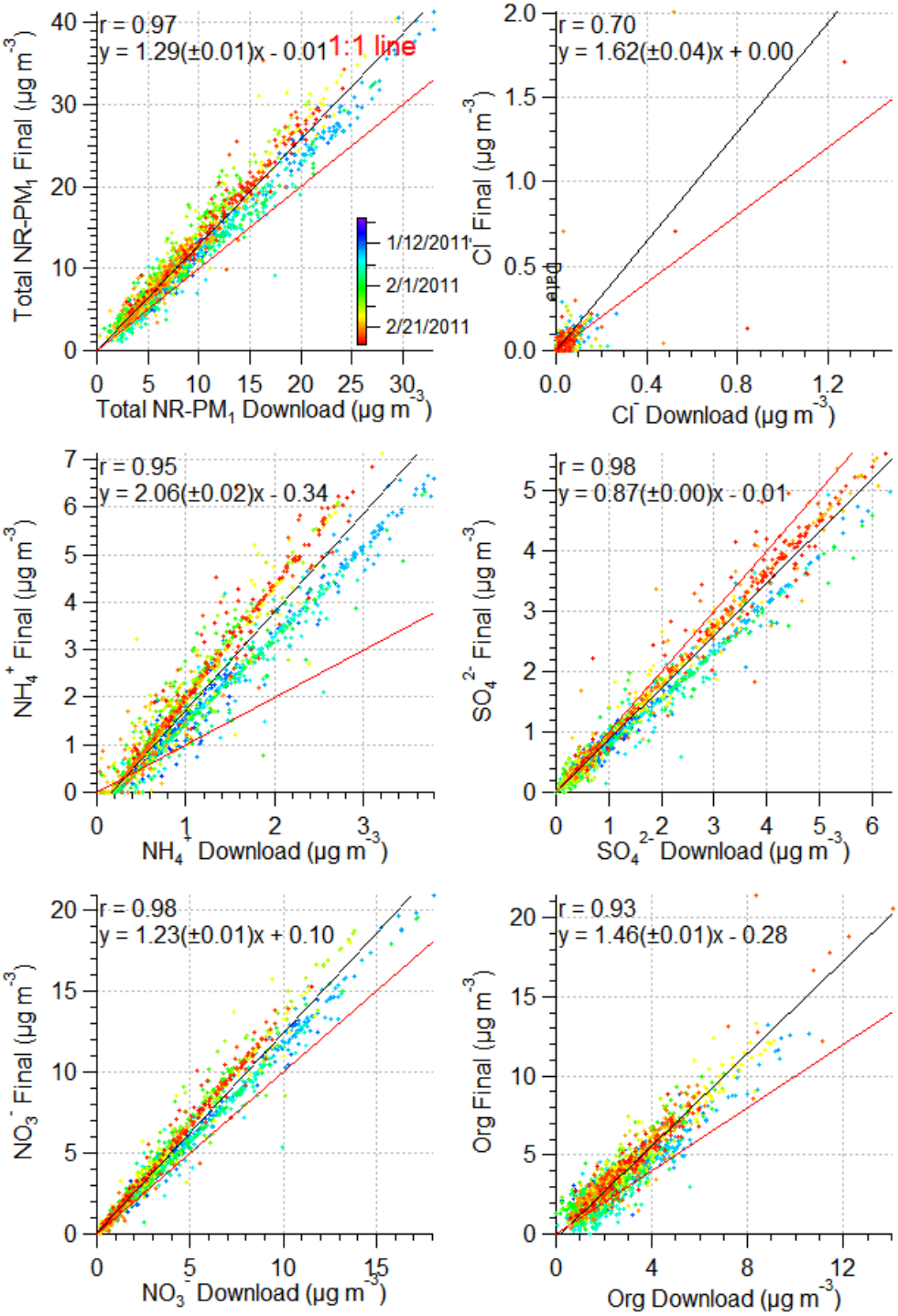

Figure 17. Correlation plots of original versus reprocessed SGP ACSM data. Plots provided by Qi Zhang.

Table 6. Slopes and correlation coefficients of the correlation plots comparing original archived data with the processed data.

Species	Slope	R^2
total NR PM_1	1.29	0.97
NH_4	2.06	0.95
NO_3	1.23	0.98
Cl	1.62	0.7
SO_4	0.87	0.98
Org	1.46	0.93

The species that are somewhat in agreement are NO_3 and SO_4. NH_4 and Org are significantly different. The Chl signal is usually near the ACSM detection limit so the correlation is a comparison of noise and is not significant. The differences are larger than should be reasonable for comparison of data from the same instrument. There is an issue with the way the two data sets were processed. These issues should be addressed by revaluation of the processed data using the data evaluation methods outlined is Section 7.0. It is clear from the discussion in Appendices 2 and 3 that reprocessing with the average calibration values and reference air beam are not sufficient to deal with the aerosol composition when high nitrate or sulfate are present.

Caroline Parworth of Qi's group also performed an analysis making monthly averages of the data. She found that in some months there was significant noise in the mas mass spectral signals where m/z>100 amu. An example is given in Figure 18. There are two possible explanations of this discrepancy. One is that it is a manifestation of the air beam correction. That is, large air-beam corrections magnify the noise but yield consistent mass concentrations. The second is that this could be an issue with the ion transmission correction applied to the reprocessed data. It also could be a combination of both reasons.

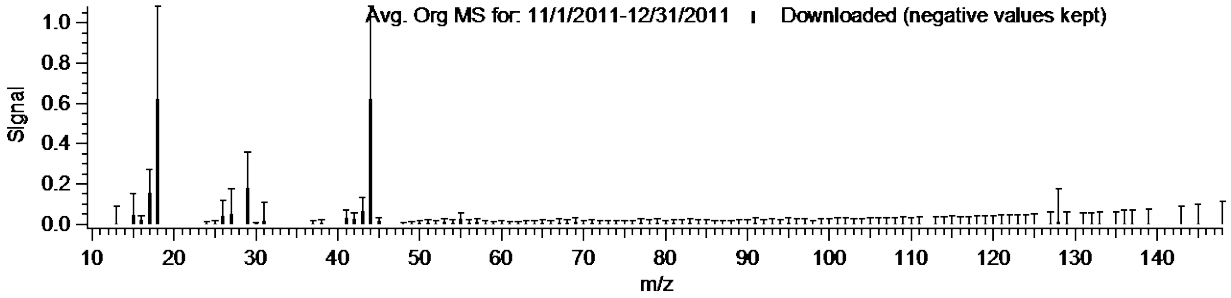

Figure 18. Average mass spectrum for 2011-11-01 to 2011-12-31. Error bars indicate 1 standard deviation. Noise increases in signals with m/z greater than 100. Plots provided by Qi Zhang.

5.3.2 Aerosol Life Cycle Intensive Operational Period (ALC-IOP) BNL 2011 Field Study

Prof. Zhang led a discussion about the ALC-IOP field program conducted at BNL in July and August 2011 during which the Mobile Aerosol Observation System (MAOS), including an ACSM s.n. 140.106, was operated along with a collocated HR-ToF-AMS from the Zhang group. Figure 19 presents correlation plots of mass loading for individual species of the ACSM data with the AMS. Slopes and correlation

coefficients are given in Table 7. Fragmentation differences between the AMS and the ACSM are one explanation for the differences in the data from the two instruments. It is not clear that the AMS and ACSM vaporizer temperatures were similar. Because the temperature measurement on the AMS vaporizer was set by adjusting the vaporizer current and is known to be inaccurate, its temperature is measured by an internal thermal couple and displayed on the front panel of the AMS electronic box. The vaporizer temperature of the AMS was also empirically checked based on the glow of the heating element. Nevertheless, a more precise check for the vaporizer temperature can be achieved based on the sodium nitrate calibration method reported in http://cires1.colorado.edu/jimenezgroup/UsrMtgs/UsersMtg11/WilliamsAMSUsersMtg_2010_VapT.pdf.

Laboratory studies by the Zhang group have determined that amine fragmentation patterns can change to some degree with vaporizer temperature and that the amine fragmentation pattern compares well with NIST pattern at low vaporizer temperature. It would be interesting to investigate whether calibration as a function of vaporizer temperature could be used to account for fragmentation differences.

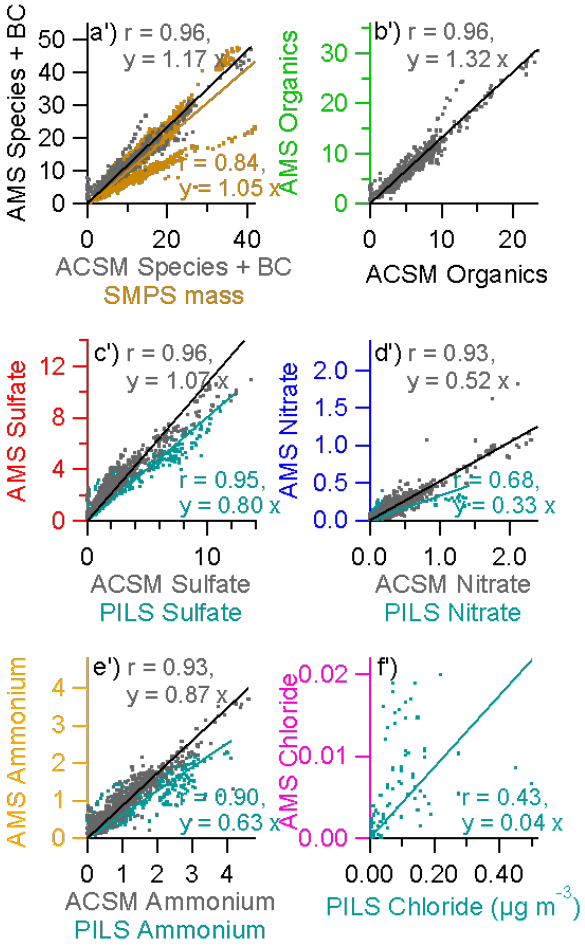

Figure 19. Correlation plots of AMS species data versus ACSM and particle-into-liquid sampler (PILS) during the ALC-IOP campaign at BNL in summer 2011. Figure copied from Zhou et al. 2016.

Table 7. Slope, intercept, and R^2 for correlation plots of AMS versus ACSM data. BC is black carbon.

Species	Slope	R^2
NR PM_1+BC	1.17	0.96
NH_4	0.87	0.93
NO_3	0.52	0.93
Cl	NA	NA
SO_4	1.07	0.96
Org	1.32	0.96

5.3.3 Mass Spectral Discrepancies between ACSM and AMS

The ACSM and AMS mass spectra for the same ambient particles show significant differences. For example, there is a significant signal at m/z 58 in the AMS mass spectra from $C_3H_8N^+$ as determined by high-resolution peak fitting (Figure 20). The $C_3H_8N^+$ signal correlates with gas-phase acetone measurements and shows a distinct time trend with elevated signal during the first half of the study (July 15-August 2, 2011) (Zhou et al. 2016). The $C_3H_8N^+$ signal disappears after 8/2/2011 (Figure 20) while acetone remains. Note that $C_2H_6O^+$ is also present at m/z 58, but its signal intensity is significantly lower than $C_3H_8N^+$, especially during the first half of the study (Figure 17). M/z 58 signal was not as prominent in the ACSM mass spectra. The ACSM cannot discriminate between $C_2H_6O^+$ and $C_3H_8N^+$ because the quadrupole mass spectrometer has unit mass resolution, significantly less than the resolution of the time-of-flight instrument. For the total signals at m/z 58 (i.e., the sum of $C_2H_6O^+$ and $C_3H_8N^+$), the ACSM signal was only 1/3 of the AMS signal.

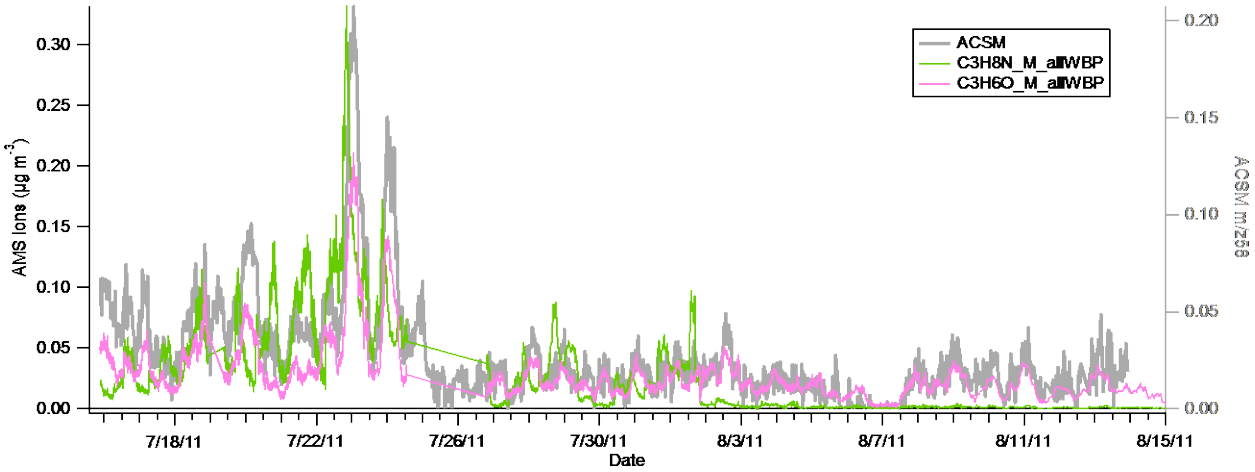

Figure 20. Time series plot of AMS ions at m/z 58 and ACSM m/z 58 signal during the ALC-IOP campaign at BNL in summer 2011.

The likely source of the m/z 58 signal is trimethylamine (TMA), a product of decomposition of plants and animals. The source of TMA during the BNL study is unknown. Like NH_3, amines are removed from the atmosphere by reactions with common atmospheric acids such as H_2SO_4 and HNO_3. But unlike NH_3, amines are also removed efficiently through rapid atmospheric oxidation reactions. The gas-phase

lifetime for TMA is estimated to be only a few hours in the troposphere based on the rates of the reaction of TMA with oxidants, such as OH, O_3, and NO_3. This suggests that the TMA source is local. As discussed in Zhou et al. (2016), the sudden disappearance of this ion after August 2, 2011 and the correlation of its signal with changes in air mass trajectory support a local source of TMA. It is possible that the source of amines is from ocean wetlands.

6.0 Data Acquisition, Data Archival, and Automated Quality Control

Connor Flynn presented an overview of the ARM data ingestion and archiving process and made recommendations to modify the ACSM datastream.

6.1 Background

ARM instruments are typically configured for autonomous operation. Local operators are responsible for day-to-day actions, daily rounds, preventative maintenance, replacement of consumables, performing some calibrations, limited trouble-shooting, problem resolution, and component replacement. The data are collected and subjected to automated quality assessment by the ARM Data Center (ADC), which also computes value-added data products and bundles the data. Data are collected hourly. The ARM Data Quality Office (DQO) produces health and status "metrics" and quicklook plots reviewed by undergraduate and masters-level students to help assess data quality and instrument health daily.

The ARM mentor is the primary contact for all issues regarding the instrument operation, health, and data quality. Mentors are expected to help define the operational practices required for operation of the instruments. They make the final call on potential problems identified by operations, the DQO, or data users. They arrange for deployments, repairs, and calibration. They are also responsible for helping define data products and assuring that the data provided to users via the ARM Data Center is of known and reasonable quality.

A schematic of the ARM data path is given in Figure 21.

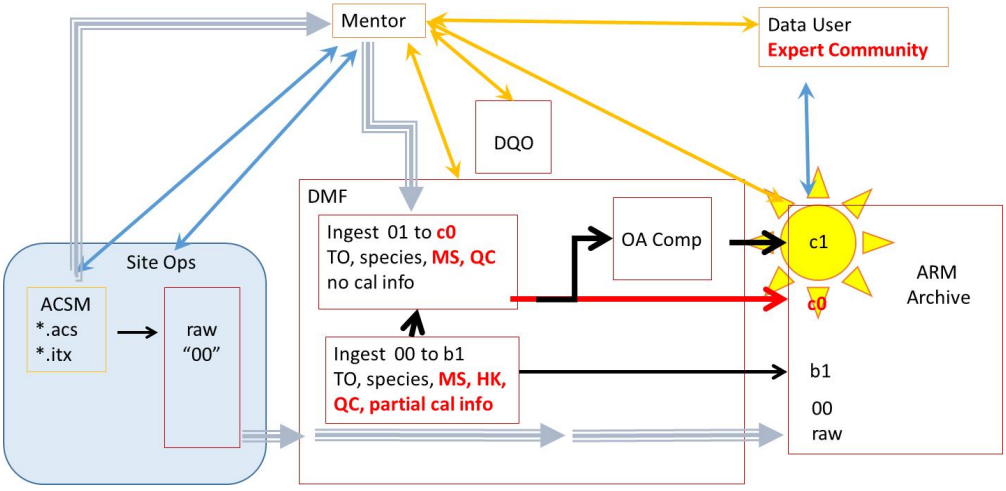

Figure 21. ARM ACSM data path.

6.2 Data Files and Archiving

Several levels of data are defined by ARM.

- 00: Raw data files
- a0: Conversion to netcdf format but no corrections applied
- a1: Application of corrections and or calibrations to yield physical units
- b1: Data evaluated by the DQO both automated and by inspection and mentor evaluation
- c1: Value-added product, either autonomously or incorporating mentor-processed data.

6.3 Data Quality Office ACSM Quality Assurance/Quality Control Methods

The DQO currently monitors ACSM inlet pressure and provides a data quality assessment. Additional checks should be added as discussed in Section 7.0.

7.0 Data Evaluation Methods

The participants determined that several methods should be incorporated into the DQO automated assessment of ACSM data.

7.1 Neutralization — Observed Ammonia to Predicted Ammonia

The first is evaluation of the ion balance. This can be accomplished by determining if the aerosol is neutralized by comparing the measured ammonium to that predicted based on the concentration of counter ions (NO_3, SO_4 and Chl).

$$NH_{4_{predicted}} = \left(\frac{2\,MW_{NH_4}}{MW_{SO_4}}\right) SO_4 + \left(\frac{MW_{NH_4}}{MW_{NO_3}}\right) NO_3 + \left(\frac{MW_{NH_4}}{MW_{Chl}}\right) Chl \P$$

Where:

$NH_{4_{predicted}} \equiv$ the predicted ammonium signal¶

$MW_s \equiv$ the molecular weight of the species s¶

$SO_4 \equiv$ the sulfate signal¶

$NO_3 \equiv$ the nitrate signal¶

$Chl \equiv$ the chloride signal¶

There should be a one-to-one slope of measured versus predicted NH_4, unless (1) there is significant organic nitrate present in the aerosol, or (2) the particulate mass is acidic (i.e., contains some fraction of

sulfuric acid that is not in a salt form). If some fraction is acidic, the correlation in the measured-versus-predicted regression line is also reduced. In general, if the correlation is strong with few outliers, the slope should be close to unity. A regression line with good correlation but non-unity slope indicates an error in collection efficiency, calibration, or relative ionization efficiency.

7.2 Volume Calculation of Mass Loading

The mass loadings of the ACSM should be compared to the mass loading determined from the SMPS and UHSAS or both. This can be done by calculating the total aerosol volume from the size distribution data obtained from these instruments and using a composition-dependent aerosol density. The fraction of each species can be determined from the fractional composition given by the ACSM. Densities for the various species are given in Table 8.

7.3 Optical Mass Loading Using Nephelometer Data

Mass loadings can be estimated from nephelometer measurements using the measured scattering coefficient and an assumption of the mass scattering efficiency where 2.5 m^2g^{-2} is a reasonable value based on an average of the literature values (Crenn, et al. 2015). The nephelometer data must be averaged over the same time intervals as the ACSM data, usually 30 minutes.

Table 8. Composition-dependent aerosol densities.

Species	Density gcm^{-3}
Organic	1.27
Cl	1.4
NO_3	1.72
NH_4	1.75
SO_4	1.78

7.4 Air Beam Magnitude

The magnitude of the air beam should also be monitored and the mentor notified if it decays from 1.0 e-7 to less than 9.0e-8.

8.0 Data Files and Archiving

The meeting developed a consensus on the content of the data files necessary to meet ARM standards.

8.1 Definitions of Data Labels for ACSM

The data stored on site by the Aerodyne data acquisition software for each of the ARM-defined data classifications are defined below.

The a0-level data should contain the raw mass spectra for each mass scan that are used to calculate the approximately 30-minute averaged files. These need to be collected directly from the DAQ software before any processing. There should be mass spectra for each filter cycle and for each sample cycle. This will require 58 mass spectra for each half-hour average. These data can be collected directly from the output of the detector.

The a1 data files should contain the automatically processed 30-minute data including the average mass spectra in the filter mode and average mass spectra in the sample mode, the average mass spectra difference between the two modes, and the calculated mass loadings for each of ammonium, nitrate, sulfate, chloride, and organics. It should also contain the parameters used to calculate the concentrations including the NO_3 response factor (RF_{NO3}), the relative ionization efficiencies for NH_4 and SO_4, the applied collection efficiency (CE), and the air beam correction factor. The version of the data acquisition software and organic sticks matrix should also be recorded in the a1 data files.

The fragmentation table should be recorded in the user's manual.

The a1-level data should contain the data after automated quality assurance (QA)/quality control (QC) processing and inspection by the DQO.

The b- level data should contain the post-processed, mentor-evaluated data — that is, the data after inspection by the mentor using the flags generated by the DQO — and should also include the organic matrix and error matrix generated by the mentor processing. Mentor processing should also include evaluation of the error matrix.

An additional C1-level datastream contains the Positive Matrix Factorization VAP) generated by the ADC.

8.2 Archiving

The current data archiving process is ad hoc and needs to be defined and made consistent. ARM needs to define the pathway for data to move through the system.

9.0 QA/QC Evaluations

Several parameters need to be evaluated to perform a thorough evaluation of the data. Some of these can be implemented by the ADC and DQO.

Selected m/z should be plotted for evaluation of the air beam: m/z 28; naphthalene, m/z 128; and baseline noise at m/z 140. Predicted ammonium, as calculated using the relationship presented in Section 7.1, versus observed ammonium should be calculated and plotted monthly. These data will identify periods that need attention when the mentor performs post-processing.

SMPS, UHSAS, or tandem differential mobility analyzer (TDMA) data, when available, should be used to calculate mass loadings using the relationships outlined in Section 7.2. The calculated mass loadings should be plotted versus total ACSM mass.

Nephelometer scattering coefficient should be used to calculate mass loading and plotted versus ACSM total mass. This should be evaluated further since significant differences have been observed in the mass loadings calculated using particle size distributions and the mass loadings calculated using the mass scattering efficiency.

Chamber background noise should be collected during calibration. This can be done by running the instrument in data collection mode with the inlet valve closed or by placing a high-efficiency particulate air (HEPA) filter in the sample stream just before the critical orifice. The equivalence of these methods should be evaluated.

10.0 Aerodyne Action Items

During the meeting it was decided to incorporate significant changes to both the data acquisition (ACSM DAQ) and analysis (ACSM Local) software. Some of these changes fit into work that is ongoing as part of a DOE Small Business Innovation Research (SBIR) Phase I project to make the ACSM more robust and autonomous and some will be in addition to that work. These recommendations will be implemented.

10.1 Changes to ACSM DAQ

1. Logging at native time resolution (i.e., ~1 minute) of raw MS and housekeeping data in addition to the current logging of averaged data (typically ~30 minutes). This data will be written by the DAQ software as Igor text (.itx) files. When ingested by ARM, these files will become the a0 data.
2. Add more calibration parameters to housekeeping data, e.g., CE, all RIEs.
3. Add logging of filament number. The instrument has two filaments, only one of which is active at any given time and each of which may have different response. Currently the DAQ is not recording which is active.
4. Lock out user from easily changing the following settings:
    a. RF Polarity
    b. Cathode voltage (electron impact voltage)

10.2 Changes to ACSM Local

There are two main focuses for changes to the ACSM Local software. First is improving the quality and completeness of the automatically calculated data. Second is to develop an export routine for post-processed data that starts from the same basic structure as the automatically exported data but extends the output to include the input data for the OACOMP VAP.

Specific tasks for automated analysis routines are as follows:

1. Improve quantification by:
    a. Automatically applying the air beam sensitivity correction
    b. Use a default CE of 0.5.

2. Add data flagging for questionable data by examining:
    a. Air beam signal
    b. Inlet pressure/flow rate
    c. Vaporizer temperature
    d. Filament emission
    e. Ionizer and vaporizer voltages
    f. Noise level at m/z 140.
3. Enhance traceability of analysis by logging:
    a. All available housekeeping data (including all applied calibration factors)
    b. Applied ion transmission correction
    c. Applied air beam correction
    d. Applied CE
    e. DAQ and analysis versions
    f. Peak integration widths
    g. Sample, filter, and difference mass spectra
    h. Speciated mass spectra.

10.3 Combined DAQ and Analysis Change

The calibration procedure that involves both the DAQ and Analysis software will also be modified. Currently, the calibration is performed in a different mode than ambient data acquisition for the sake of speed. This works well in general, but in some cases a slow response from SO_4 can lead to differences between SO_4 RIE measured in this mode compared with that in the slower mode we run for normal data acquisition. To that end the calibration procedure will be modified to use the same scanning mode as the standard data acquisition.

11.0 Points for Discussion at the Second Users' Meeting

11.1 PMF Data Processing

The best diagnostic of the error matrix is the value at which the standard deviation of the average signal at the individual m/z, Q, divided by the standard deviation at a mass where there is no mass loading, Q-expected or Q/Q-expected from the PMF analysis, converges. This value should be close to one. This evaluation has been made in several ways prior to implementation of Principal Matrix Factorization (PMF). A tool is built into the ACSM error exporting routine to compare the calculated uncertainty to the standard deviation of data collected during periods when the point-to-point signal variation is a result of noise rather than actual changes in loading. This is somewhat subjective. Another approach, built into the ACSM analysis software, is the application of a smoothing routine to the mass loading data. The

difference between the raw and smoothed data is then calculated and compared to the calculated uncertainties.

11.2 Qi Zhang Data Reprocessing Evaluation

The data used by Professor Zhang should be evaluated specifically after application of calibration and AB corrections described above and the data changes evaluated.

11.3 HI-SCALE

Specific attention to the HI-SCALE IOP data is necessary. The comparison at Aerodyne revealed several questions:

- Why is the A1 presented in the Fast plots significantly less noisy than the data we evaluated during the meeting? Is Fast org A1 data de-spiked?
- A 30% difference between ACSM and AMS is within the expected range of agreement between the two instruments because overall uncertainty is ~30%. Why are the organic mass loadings significantly greater than this? The evaluation of the AMS MS and the processing methods are needed to determine why there is a difference in the organic mass loadings.
- How were the SMPS data worked up by PNNL? Which density was used by Fast et al.?

11.4 ACSM Data Processing

Now that the SGP ACSM historical data has been evaluated and reprocessed, we will turn our attention to other DOE ACSM data sets of specific interest, including:

- HI-SCALE Reanalysis
- SGP ACSM AMF7 Winter 2016-2017
- SGP ACSM AMF7 2017
- ASI 2017
- ENA 2017.

12.0 References

Aiken, AC, PF DeCarlo, JH Kroll, DR Worsnop, JA Huffman, KS Docherty, IM Ulbrich, C Mohr, JR Kimmel, D Sueper, Y Sun, Q Zhang, A Trimborn, M Northway, PJ Ziemann, MR Canagratna, TB Onasch, M Rami Alfarra, ASH Prévôt, J Dommen, J Duplissy, A Metzger, U Baltensperger, and JL Jimenez. 2008. "O/C and OM/OC Ratios of Primary, Secondary, and Ambient Organic Aerosols with High-Resolution Time-of-Flight Aerosol Mass Spectrometry." *Environmental Science and Technology* 42(12): 4478-4485, doi:10.1021/es703009q.

Allan, JD, AE Delia, H Coe, KN Bower, M Rami Alfarra, JL Jimenez, AM Middlebrook, F Drewnick, TB Onasch, MR Canagaratna, JT Jayne, and DR Worsnop. 2004. "A generalized method for the extraction of chemically resolved mass spectra from Aerodyne aerosol mass spectrometer data." *Journal of Aerosol Science* 35(7): 909-922, doi:10.1016/j.jaerosci.2004.02.007.

Rami Alfarra, M, H Coe, JD Allan, KN Bower, H Boudries, MR Canagaratna, JL Jimenez, JT Jayne, AA Garforth, S Li, and DR Worsnop. 2004. "Characterization of urban and rural organic particulate in the Lower Fraser Valley using two Aerodyne Aerosol Mass Spectrometers." *Atmospheric Environment* 38(34): 5745-5758, doi:10.1016/j.atmosenv.2004.01.054.

Crenn. V, J Sciare, PL Croteau, S Verlha, R Fröhlich, CA Belis, W Aas, M Äijälä, A Alastuey, B Artiñano, D Baisnée, N Bonnair, M Bressi, M Canagaratna, F Canonaco, C Carbone, F Cavalli, E Coz, MJ Cubison, JK Esser-Gietl, DC Green, V Gros, L Heikkinen, H Herrmann, C Lunder, MC Minguillón, G Mocnik, CD O'Dowd, J Ovadnevaite, J-E Petit, E Petralia, L Poulain, M Priestman, V Riffault, A Ripoll, R Sarda-Estève, JG Slowik, A Setyan, A Wiedensohler, U Baltensperger, ASH Prévôt, JT Jayne, and O Favez. 2015. "ACTRIS ACSM intercomparison – Part 1: Reproducibility of concentration and fragment results from 13 individual Quadrupole Aerosol Chemical Speciation Monitors (Q-ACSM) and consistency with co-located instruments." *Atmospheric Measurement Techniques* 8(12): 5063-5087, doi:10.5194/amt-8-5063-2015.

Middlebrook, AM, R Bahreini, JL Jimenez, and MR Canagaratna. 2012. "Evaluation of Composition-Dependent Collection Efficiencies for the Aerodyne Aerosol Mass Spectrometer using Field Data." *Aerosol Science and Technology* 46(3): 258-271, doi:10.1080/02786826.2011.620041.

Parworth, C, J Fast, F Mei, T Shippert, C Sivaraman, A Tilp, T Watson, and Q Zhang. 2015. "Long-term measurements of submicrometer aerosol chemistry at the Southern Great Plains (SGP) using an Aerosol Chemical Speciation Monitor (ACSM)." *Atmospheric Environment* 106: 43-55, doi:10.1016/j.atmosenv.2015.01.060.

Pieber, SM, I El Haddad, JG Slowik, MR Canagaratna, JT Jayne, SM Platt, C Bozzetti, KR Daellenbach, R Fröhlich, A Vlachou, F Klein, J Dommen, B Miljevic, JL Jimenez, DR Worsnop, U Baltensperger, and ASH Prévôt. 2016. "Inorganic Salt Interference on CO_2^+ in Aerodyne AMS and ACSM Organic Aerosol Composition Studies." *Environmental Science and Technology* 50(19): 10494-10503, doi:10.1021/acs.est.6b01035.

Zhou, S, S Collier, J Xu, F Mei, J Wang, Y-N Lee, AJ Sedlacek, SR Springston, Y Sun, and Q Zhang. 2016. "Influences of upwind emission sources and atmospheric processing on aerosol chemistry and properties at a rural location in the Northeastern U.S." *Journal of Geophysical Research – Atmospheres* 121(10): 6049-6065, doi:10.1002/2015JD024568.

Appendix A

HI-SCALE Reanalysis

The HI-SCALE data were reanalyzed using the average calibration values presented in Table 2. Time series for both IOPs are presented in Figure 22 and Figure 25. Correlation plots of total ACSM mass versus mass calculated from SMPS volume data are presented in Figure 23 and Figure 24 for IOP 1 and Figure 26 and Figure 27 for IOP 2. The first figure in each series (Figure 23 and Figure 26) shows linear orthogonal fits including an intercept. The second figure in each series (Figure 24 and Figure 27) shows orthogonal fits with intercept forced through zero. SMPS data are courtesy of John Shilling, PNNL.

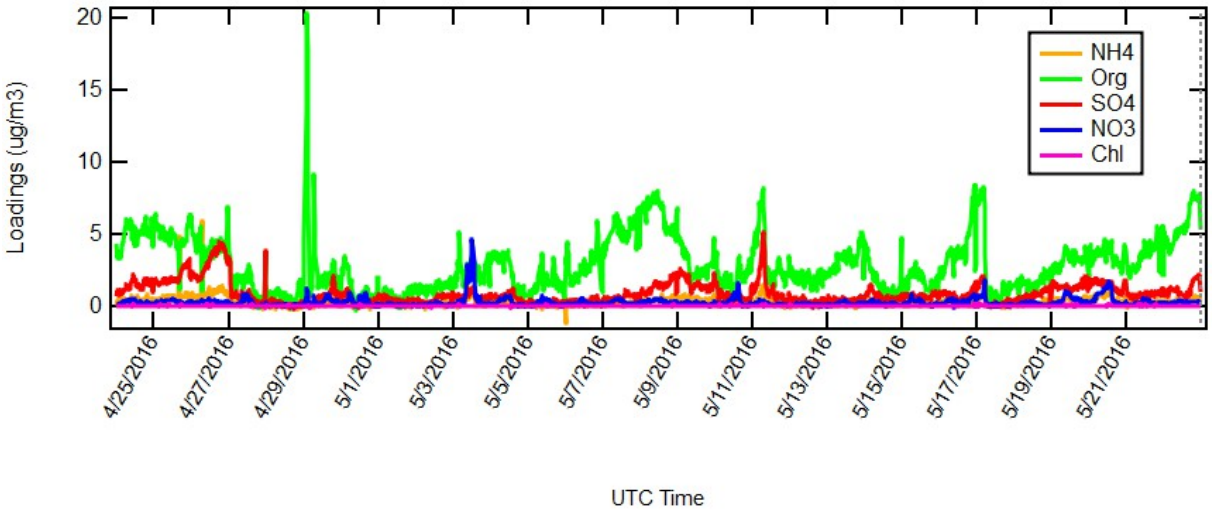

Figure 22. HI-Scale IOP 1 SGP ACSM time series data processed using the average calibration values over the seven-year history of SGP ACSM operation.

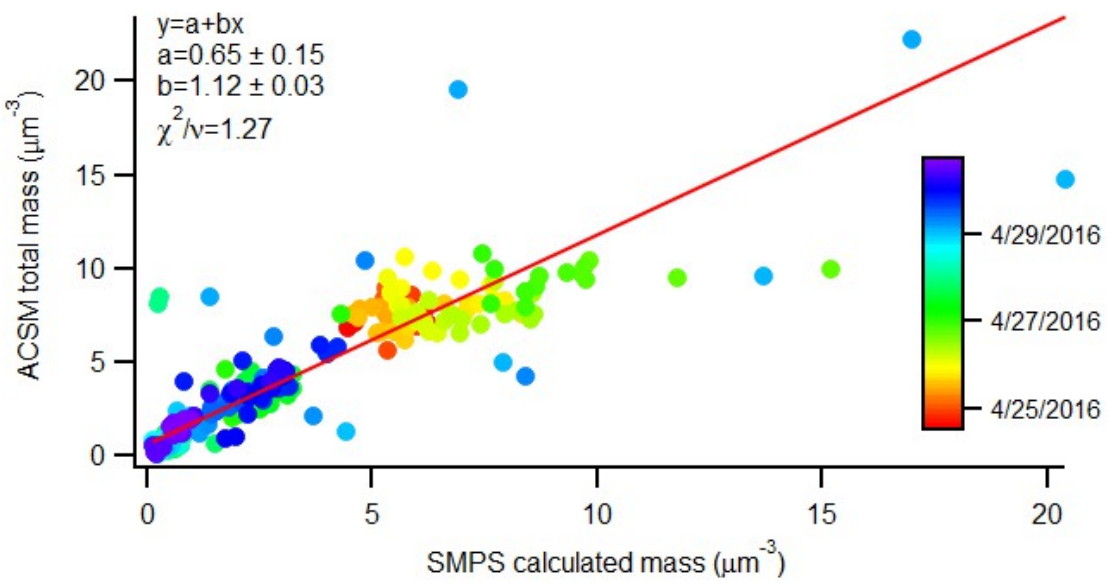

Figure 23. Correlation plot of IOP 1 ACSM-measured total mass with mass calculated from ground-based SMPS size distribution. The fit is an orthogonal distance regression.

The correlation plots show good agreement between the ACSM-measured mass loading and the mass loading calculated from the SMPS data with a slope of 1.12 and an intercept of.0.65 µg m^{-3}. The reason for the intercept is not clear.

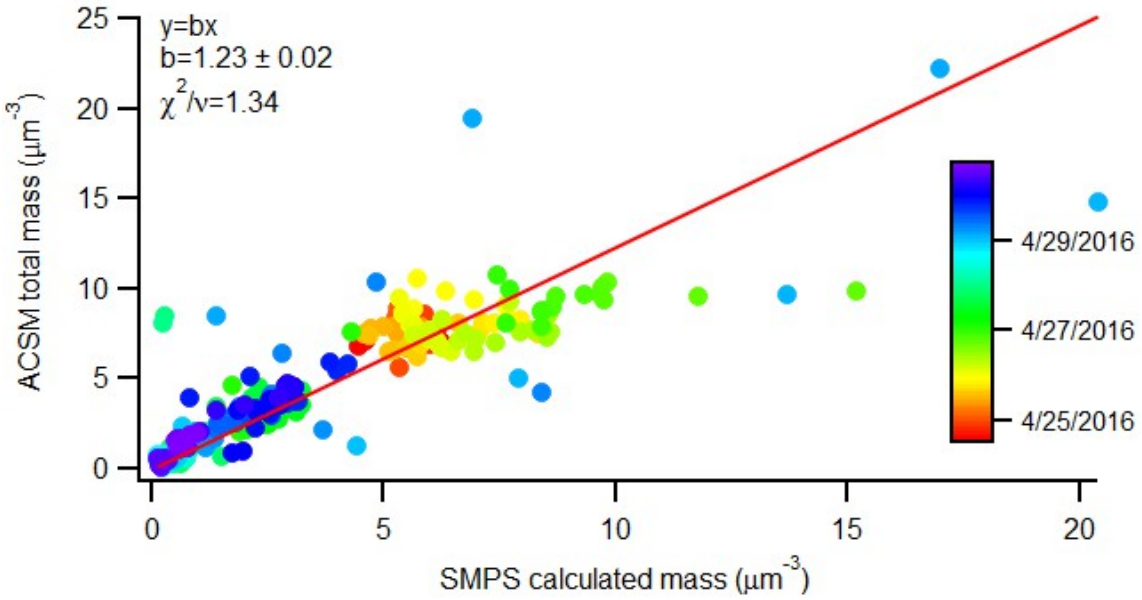

Figure 24. Correlation plot of IOP 1 ACSM-measured total mass with mass calculated from ground-based SMPS size distribution. The fit is an orthogonal distance regression forced through zero.

The correlation plots forced through zero show good agreement between the ACSM-measured mass loading and the mass loading calculated from the SMPS data with a slope of 1.23.

The time series of ACSM mass loading data are presented in Figure 25. The data gap is the result of a filter valve switching problem.

The correlation plots (Figure 26 and Figure 27) show good agreement between the ACSM-measured mass loading and the mass loading calculated from the SMPS data with a slope of 1.18 and an intercept of.0.99 μg m^{-3}. The reason for the intercept is not clear. The reason for the intercepts is likely a result of the noise in both the ACSM and SMPS signals and should be a topic of discussion for the next users' meeting.

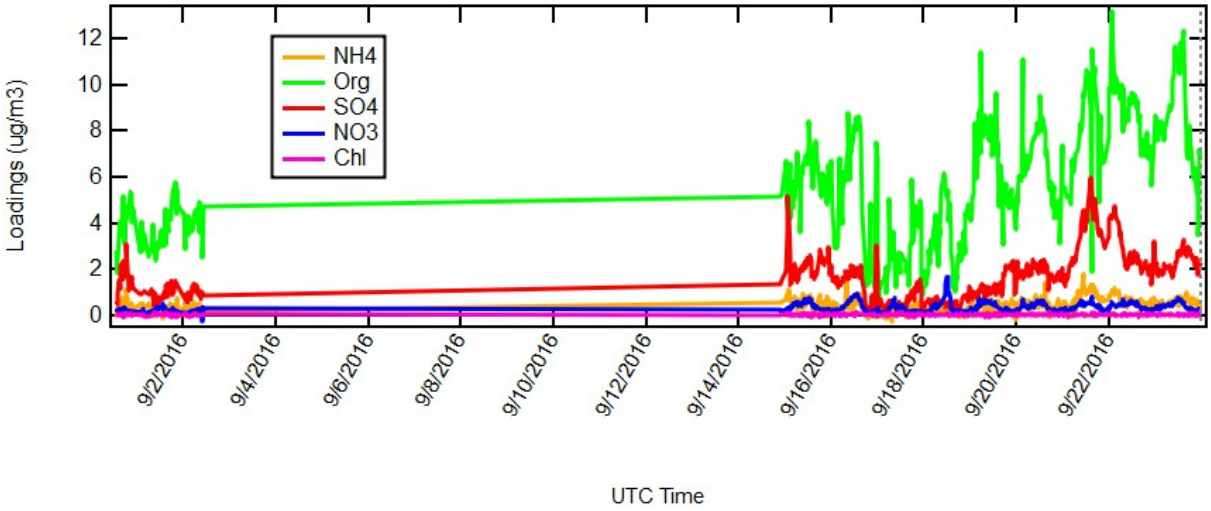

Figure 25. HI-Scale IOP 2 SGP ACSM time series. The data gap is because the filter switching valve was out of adjustment causing low inlet pressure in the sample position.

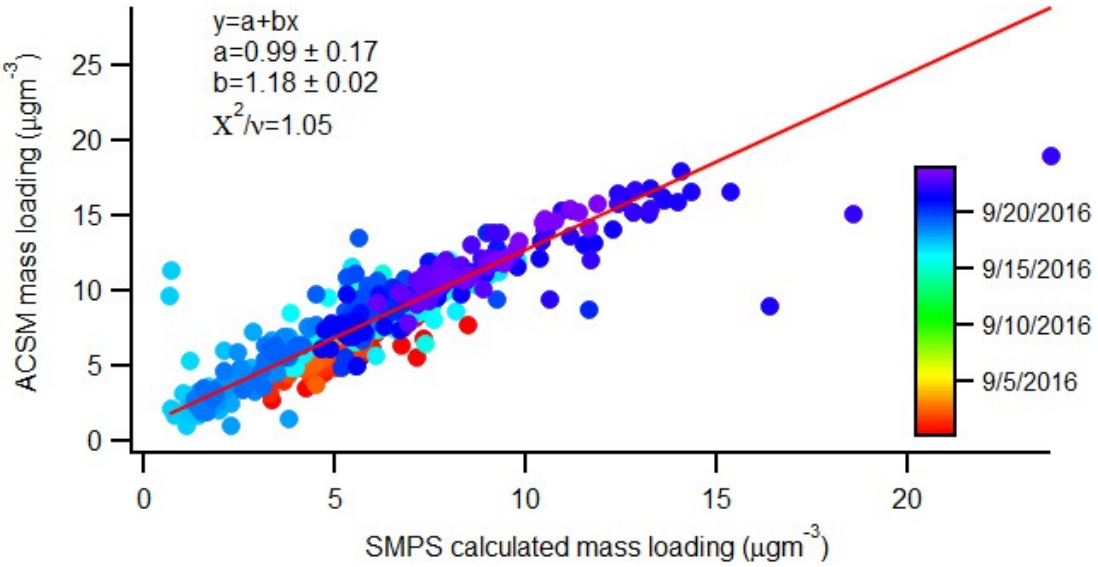

Figure 26. Correlation plot of IOP 2 ACSM-measured total mass with mass calculated from ground-based SMPS size distribution. The fit is an orthogonal distance regression.

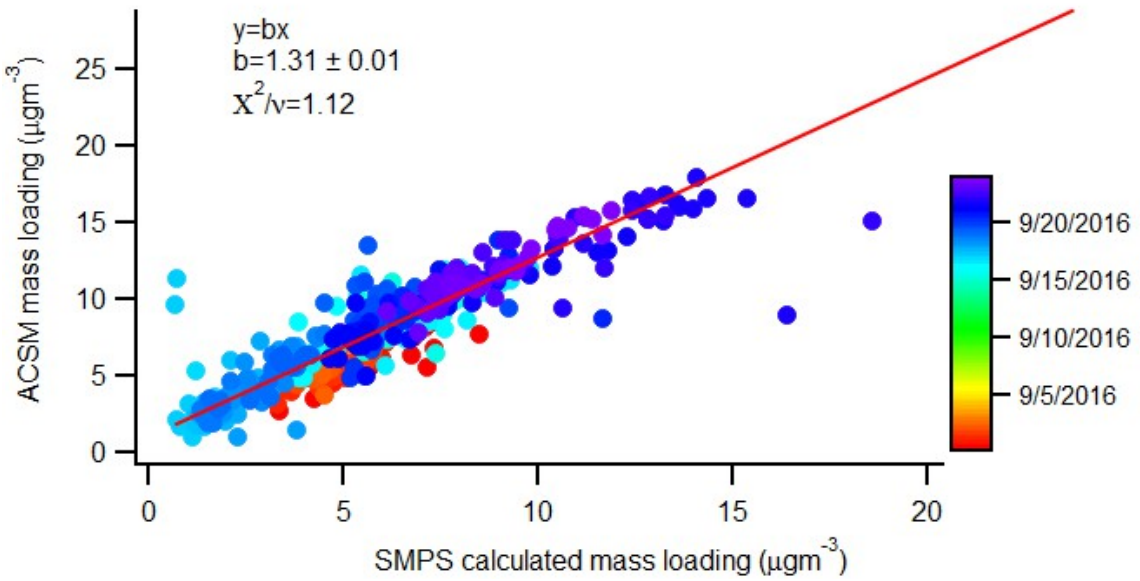

Figure 27. Correlation plot of IOP 2 ACSM-measured total mass with mass calculated from ground-based SMPS size distribution. The fit is an orthogonal distance regression forced through zero.

www.arm.gov

U.S. DEPARTMENT OF
ENERGY

Office of Science